ENVIRONMENTAL RESEARCH

LETTERS

LETTER • OPEN ACCESS

Observation of aerosol induced 'lower tropospheric cooling' over Indian core monsoon region

To cite this article: Manish Jangid et al 2021 Environ. Res. Lett. 16 124057

View the <u>article online</u> for updates and enhancements.

You may also like

- Reduction of mid-summer rainfall in northern India after the late-1990s induced by the decadal change of the Silk Road pattern Xi Wang, Riyu Lu and Xiaowei Hong
- Seasonal tropospheric cooling in Northeast China associated with cropland expansion
- Yaqian He, Eungul Lee and Justin S Mankin
- Contrasting interannual impacts of European and Greenland blockings on the winter North Atlantic storm track Minghao Yang, Dehai Luo, Weilai Shi et

ENVIRONMENTAL RESEARCH

LETTERS



OPEN ACCESS

RECEIVED

5 August 2021

REVISED

17 November 2021

ACCEPTED FOR PUBLICATION

19 November 2021

PUBLISHED

10 December 2021

Original content from this work may be used under the terms of the Creative Commons Attribution 4.0 licence.

Any further distribution of this work must maintain attribution to the author(s) and the title of the work, journal citation and DOI.



LETTER

Observation of aerosol induced 'lower tropospheric cooling' over Indian core monsoon region

Manish Jangid¹, Amit Kumar Mishra^{1,*}, Ilan Koren², Chandan Sarangi³, Krishan Kumar¹, Sachchidanand Singh⁴ and Sachchidanand Tripathi⁵

- School of Environmental Sciences, Jawaharlal Nehru University, New Delhi 110067, India
- ² Depratment of Earth and Planetary Sciences, Weizmann Institute of Sciences, Rehovot 7610001, Israel
- ³ Department of Civil Engineering, Indian Institute of Technology, Madras, Tamil Nadu 600036, India
- Environmetal Science and Biomedical Metrology Division, CSIR-National Physical Laboratory, New Delhi 110012, India
- Department of Civil Engineering, Indian Institute of Technology, Kanpur, Uttar Pradesh 208016, India
- * Author to whom any correspondence should be addressed.

E-mail: amit.mishra.jnu@gmail.com

Keywords: aerosols, clouds, radiative effect, lower tropospheric stability, Indian subcontinent

Supplementary material for this article is available online

Abstract

Aerosols play a significant role in regional scale pollution that alters the cloud formation process, radiation budget, and climate. Here, using long-term (2003–2019) observations from multi-satellite and ground-based remote sensors, we show robust aerosol-induced instantaneous daytime lower tropospheric cooling during the pre-monsoon season over the Indian core monsoon region (ICMR). Quantitatively, an average cooling of $-0.82\,^{\circ}\text{C} \pm 0.11\,^{\circ}\text{C}$ to $-1.84\,^{\circ}\text{C} \pm 0.25\,^{\circ}\text{C}$ is observed in the lower troposphere. The observed cooling is associated with both aerosol-radiation and aerosol-cloud-radiation interaction processes. The elevated dust and polluted-dust layers cause extinction of the incoming solar radiation, thereby decreasing the lower tropospheric temperature. The aerosol-cloud interactions also contribute to enhancement of cloud fraction which further contributes to the lower tropospheric cooling. The observed cooling results in a stable lower tropospheric structure during polluted conditions, which can also feedback to cloud systems. Our findings suggest that aerosol induced lower tropospheric cooling can strongly affect the cloud distribution and circulation dynamics over the ICMR, a region of immense hydroclimatic importance.

1. Introduction

Aerosols have significant implications on global as well as regional climate (Ramanathan and Crutzen 2003, Li et al 2016a). They play an important role in radiation budget due to scattering and absorption of the incoming and outgoing solar radiation (Ramanathan and Feng 2009, Boucher et al 2013, Zhao et al 2020), which depend on the physicochemical properties of aerosols (Tripathi et al 2005a, Singh et al 2010). Also, aerosols provide a viable surface for droplet nucleation and thus play a significant role in cloud formation processes (Twomey 1977, Koren et al 2008), and thereby further participate in radiation balance (Albrecht 1989, Garrett and Zhao 2006). Over the last few decades, rising population, industrialization and transportation have

contributed immensely to the tropospheric pollution over developing countries (Gargava and Aggarwal 1996, Ramanathan and Parikh 1999, Kandlikar and Ramachandran 2000, Tripathi *et al* 2005b). Being close to the Earth's surface, troposphere is the most affected atmospheric layer due to emissions from anthropogenic and natural sources. The physical processes related to mass and energy transfer near the surface make the air pollution-cloud-radiation interactions more complex, which further necessitates the importance of studying these interactions.

The monsoon system over the Asian region is strongly associated with changes in pre-monsoonal and monsoonal aerosol loading (Lau and Kim 2006, Ganguly *et al* 2012, Li *et al* 2016b). A three-fold increase in atmospheric aerosols is witnessed during the pre-monsoon season over Asia since the late

1990s (Kulkarni et al 2008, Vernier et al 2015). The Indian subcontinent, particularly the northern and eastern part has experienced a sustained aerosol load in the last two decades (Kuttippurath and Raj 2021, Mhawish et al 2021). These elevated pollution layers are mainly dominated by dust and polluted-dust (mixed) during the pre-monsoon season (Mishra and Shibata 2012, Sarangi et al 2016). These aerosols have a considerable radiative impact on the monsoon system (Lau and Kim 2006, Lau et al 2006, Höpner et al 2019, Krishnamohan et al 2021). Recent hypotheses on aerosol-radiation-monsoon interactions highlight the importance of physico-chemical properties and vertical distribution of aerosols in troposphere (Ramanathan et al 2005, Lau and Kim 2006, Nigam and Bollasina 2010, D'Errico et al 2015). The elevated heat pump hypothesis postulates that elevated absorbing aerosols over the Southern slope of Himalayas and Tibetan Plateau heat the atmospheric layer and assist in strengthening the monsoonal wind prior to the normal onset period (Lau and Kim 2006, Lau et al 2006). This hypothesis has been debated by several studies (Nigam and Bollasina 2010, Wonsick et al 2014, D'Errico et al 2015, Kovilakam and Mahajan 2016). Another hypothesis related to widespread absorbing brown clouds over northern Indian Ocean suggests that aerosol induced surface cooling may weaken the monsoon strength (Ramanathan 2004, Ramanathan et al 2005). Further, aerosol-induced changes in cloud properties over regional scale can modulate the temperature structure and play a significant role in lower tropospheric turbulence in warmer and more polluted regions (Kothawale and Kumar 2002, Fu et al 2004). These different space-time dependent mechanisms associated with aerosol-cloud-monsoon interactions highlight the need to understand the radiative impact of pre-monsoonal pollution loading on atmospheric thermal profiles.

Sarangi et al (2016) have shown that the elevated aerosols are associated with radiative cooling near surface layers during monsoon onset period (a short time window) over Kanpur, a city located in the Indo-Gangetic Plain (IGP). They suggest that vertical positioning of aerosol layers and their extinction properties are major contributors to this cooling. Similar findings have been found over other regions, such as Beijing China (Guo et al 2020), indicating that this is a robust mechanism. In another study based on numerical model simulations and satellite data, Sarangi et al (2018) report that aerosol induced cloud invigoration during monsoon period causes cooling at both the surface and top of the atmosphere (TOA). This cooling is primarily caused by cloud brightening associated with changes in macro- and microphysical properties of clouds. These studies underline the importance of aerosol induced changes in radiation budget at different spatio-temporal scales. However, the above discussed previous studies have not explicitly illustrated the sensitivity of temperature profiles to net aerosol effects (both direct and indirect) on regional scale through observations over the Indian subcontinent, to the best of our knowledge. Thus, the variations in temperature profiles as a function of aerosol loading and cloud changes need to be investigated on a regional scale.

Although, significant increasing trends (0.17 °C/decade–0.19 °C/decade) have been observed in annual mean surface temperature over the northern and southern parts of India (Thomas et al 2019). Similar trends are absent over the central and northeastern parts (a significant portion of the Indian core monsoon region (ICMR)) of India during the premonsoon season (Ross et al 2018). They hypothesize that the prevalent absorbing brownish haze is the main reason for the observed surface cooling over the ICMR. Further, they claim that absorbing aerosol induced heating aloft and resultant cooling at surface, may bring dynamical changes in this region. However, the trends in temperature of lower tropospheric region are not clear. The above-mentioned surface temperature anomaly and related hypothesis over the ICMR warrants deeper investigation on this subject. The present study aims to examine the role of aerosol direct and indirect effect on tropospheric thermal profiles using 17 years multi-satellite and groundbased observations over the ICMR during the premonsoon period. Further, the impact of clouds on the aerosol-induced changes in tropospheric thermal structure and their associations are also investigated.

2. Data and methods

Aerosol types are characterized using ground-based remote sensors of Aerosol Robotic NETwork (AER-ONET) located in the ICMR (here we have taken 21° N-27° N; 80° E-90° E; figure 1(a)), over the central and northeastern part of India (Saha et al 2014). ICMR includes four AERONET stations namely Kanpur (KNP), Gandhi College Patna (GC), Kolkata (KOL), and Dhaka University (DHK), shown as black colored dots inside a rectangular box (figure 1(a)). AERONET level 2.0 data of aerosol optical depth (AOD), absorbing AOD (AAOD), single scattering albedo (SSA) and volume size distribution (Holben et al 1998) during the pre-monsoon season (March, April, May) are used in this study. The AOD and AAOD at 500 nm (AOD500, and AAOD500) are calculated with the help of Angstrom exponent (AE) and absorption Angstrom exponent (AAE) measurements at 440 and 870 nm (Smirnov et al 2002, Soni et al 2011, Jangid et al 2019). The aerosol types are characterized based on AE and AAE. It is classified into four types based on the following (AE, AAE) classification: (a) dust (≤ 0.8 , ≥ 1.8), (b) biomass burning aerosols (≥ 1.2 , ≥ 1.8), (c) urban/industrial aerosols

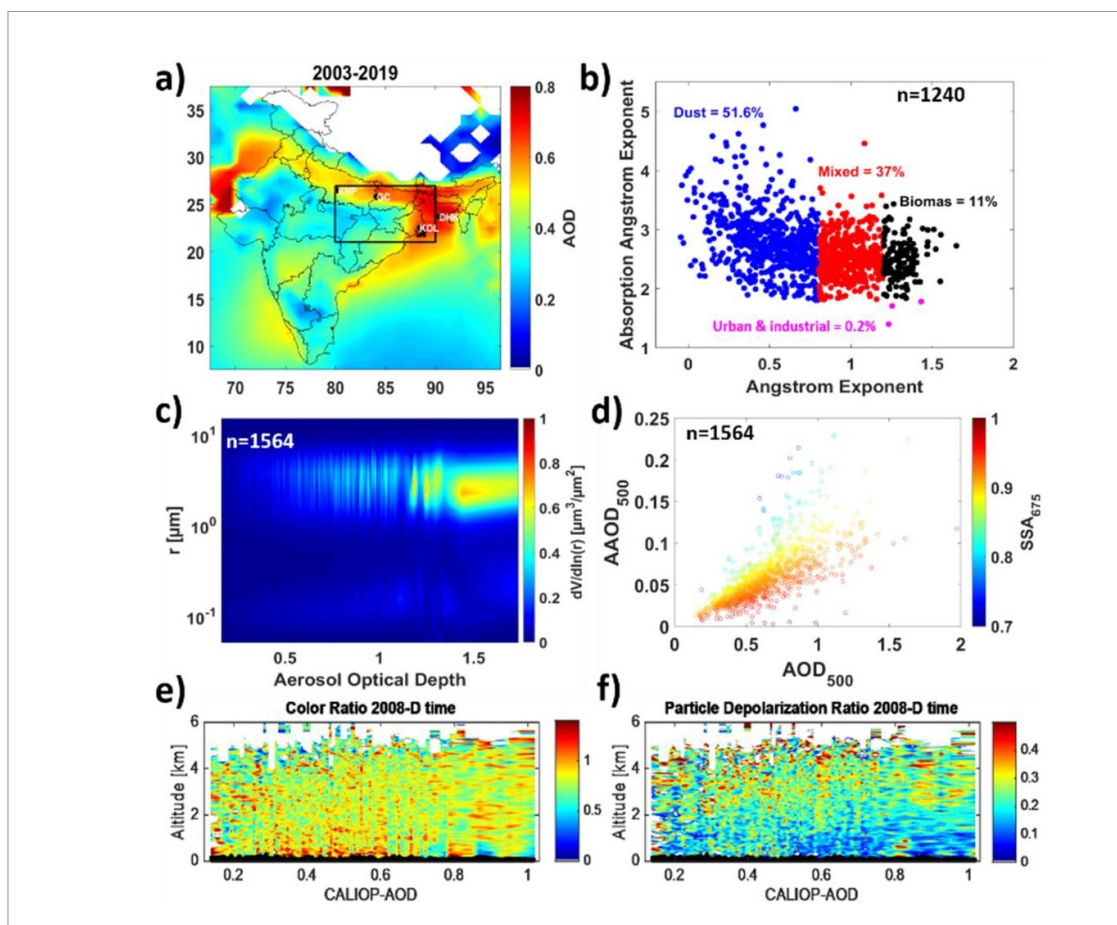


Figure 1. (a) Spatial distribution of MODIS derived daily mean AOD climatology (2003–2019) during pre-monsoon season. Black dots show the location of four AERONET stations (Kanpur (KNP), Gandhi College Patna (GC), Kolkata (KOL), Dhaka University (DHK)) inside the rectangular black box, which shows the boundary of the ICMR used in this study. (b) Scatter plot representing aerosol types based on AE and AAE, (c) volume particle size distribution $(dV(r)/dlnr (\mu m^3/\mu m^2))$, and (d) AAOD and SSA as a function of AOD during pre-monsoon season (2003–2019) using AERONET data. CALIOP-derived vertical distribution of (e) color ratio and (f) particle depolarization ratio as a function of AOD for the year 2008 over the ICMR during the pre-monsoon season. The total number of data samples used in various analyses are shown as 'n' in respective plots.

(\geqslant 1.2, <1.8), and rest as (d) mixed aerosols (Russell *et al* 2010, Giles *et al* 2012, Jangid *et al* 2019).

Particle extinction and backscatter coefficient at 532 nm and 1064 nm, and two polarization planes at 532 nm derived from Cloud-Aerosol Lidar with Orthogonal Polarization (CALIOP) level 2 Ver. 3.01 on board the Cloud-Aerosol Lidar and Infrared Pathfinder Satellite Observations (CALIPSO) are used for analysis of the vertical profiles of aerosol (Winker et al 2003, 2007, Young et al 2008, Young and Vaughan 2009). The ratio of backscatter coefficient at 1064 nm to that at 532 nm is known as the color ratio, an indicator for size of aerosols. Particle depolarization ratio is the ratio of perpendicular to parallel backscatter coefficient (Cairo et al 1999), which tells about the shape of particles; higher values indicate dominance of non-spherical particles. The integrated extinction profile at 532 nm is used to estimate aerosol optical depth from CALIOP. Additional information on the CALIOP aerosol identification algorithm and aerosol products are provided by Omar et al (2009).

The Moderate Resolution Imaging Spectroradiometer (MODIS) and Atmospheric InfraRed Sounder (AIRS) onboard Aqua satellite provide daily averaged columnar AOD (at 550 nm) and vertical profiles of temperature, respectively. The MODIS derived AOD (collection 6.1) and AIRS derived (Aqua overpass time \sim 13:30 LT) daily temperature profiles $(T_{\rm day})$ at six pressure levels (surface, 925, 850, 700, 600, and 500 hPa) are used to analyze the effect of aerosol on tropospheric temperature profiles during the pre-monsoon season for 17 years (2003-2019). It is important to mention that the AIRS retrievals of temperature profiles are strongly related to average kernel functions used in algorithms (Maddy et al 2008). In other words, the temperature corresponding to the denoted pressure levels actually is the temperature of an atmospheric layer around those specific pressure levels. AIRS temperature retrievals have been compared and validated against radiosonde data during hazy and cloudy conditions, and are found satisfactory (Davidi et al 2009 and references therein). The spatial resolution of MODIS and AIRS data used in this study is $1^{\circ} \times 1^{\circ}$. The method used here to estimate aerosol-induced temperature perturbation (refer supplementary note (SN) 1 (available online at stacks.iop.org/ERL/16/124057/mmedia)) is also previously used over many regions across the world (Davidi *et al* 2009, 2012, Mishra *et al* 2014).

The space-borne Clouds and the Earth's Radiant Energy System (CERES) SYN1 deg derived daily short-wave (SW) and long-wave (LW) downwelling radiation fluxes at the surface (SRF) and upwelling radiation fluxes at the TOA in both clearsky ($F_{\text{clear-sky}}$) and all-sky ($F_{\text{all-sky}}$) condition at $1^{\circ} \times 1^{\circ}$ spatial resolution (Loeb et al 2018) are used for analysis of variation in radiation fluxes (SW and LW) with AOD. Cloud fraction (CF) and AOD derived from CERES SSF1deg data that are generated from MODIS (Smith et al 2012) are used in this study. The changes in downwelling radiation fluxes due to clouds are calculated by the difference between $F_{\text{all-sky}}$ and F_{clear-sky} in both LW and SW at SRF, termed as cloud radiative effect at SRF (CRE-SRF) (e.g. Sarangi et al 2018, Kang et al 2020). The difference between upwelling $F_{\text{clear-sky}}$ and $F_{\text{all-sky}}$ at TOA in both SW and LW regime is termed as CRE at the TOA (CRE-TOA) (e.g. Shupe and Intrieri 2004, Feingold et al 2016, Stapf et al 2020).

Aqua-MODIS derived $1^{\circ} \times 1^{\circ}$ gridded daily averaged CF, cloud top pressure (CTP) and cloud optical thickness (COT) are used for International Satellite Cloud Climatology Project (ISCCP) cloud-types classification, which classifies clouds into nine different categories (Rossow and Schiffer 1991, Kumar and Bhat 2016, Liang *et al* 2017, Sarangi *et al* 2018). The nine different types of clouds are as follows: (a) cumulus (Cu), (b) stratocumulus (Scu), and (c) stratus (St) are low-level clouds; (d) altocumulus (ACu), (e) altostratus (ASt), and (f) nimbostratus (NSt) are middle-level clouds; and (i) cirrus (Ci), (j) cirrostratus (CiSt), and (k) deep convective clouds (DCC) are high-level clouds.

Our cloud classification scheme shows CF \sim 0–0.5 as a more common sky condition (hereafter used as ambient sky condition) over the study region during pre-monsoon season. Moreover, sampling with CF greater than 0.5 during this period may introduce significant artefacts in aerosol retrievals. As such, we have only taken CF in the range of 0–0.5 for our study, which constitutes 80% of the total data. The methods of analysis pertaining to change in $T_{\rm day}$ per unit AOD (d $T/{\rm d}\tau$) and cloud frequency as a function of CF and AOD respectively, are provided in SN2.

3. Results and discussion

3.1. Aerosol characterization over the ICMR

Figure 1(b) shows the percentage composition of aerosol types based on AE and AAE datasets during the pre-monsoon season. It shows the dominance of dust type aerosols (51.6%) followed by a mixed type

of aerosols (37%). The major sources of these dust particles in pre-monsoon are from the western desert region (Gautam *et al* 2011, Pandey *et al* 2017). These dust aerosols further mix with local pollutants to form the polluted-dust (mixed) over the downwind region. The aerosols categorization based upon a similar algorithm over the Indian region has been reported by various studies (Giles *et al* 2012, Kaskaoutis *et al* 2012, Jangid *et al* 2019).

Figure 1(c) represents a contour plot of volume particle size distribution as a function of aerosol particle radius and AOD, showing increase in coarse mode (radius $> 1 \mu m$) aerosol concentration with the increase in aerosol loading. In other words, coarser particles dominate higher AOD which are mostly dust and polluted-dust aerosols. Figure 1(d) shows a 2D scatter plot of AOD, AAOD and SSA, where the colorbar represents SSA. It shows a positive association between AOD and AAOD with SSA <0.92 (~70% of total data). In other words, the increase in absorption fraction is associated with increase in total extinction. It indicates that the pre-monsoonal aerosols are mostly absorbing in nature (SSA <0.92). Figures 1(e) and (f) show the dominance of larger (high color ratio values) and non-spherical (high particle depolarization ratio values) particles between 1-4 km altitude range.

The observed properties of aerosols in a high aerosol loading environment indicate the dominance of elevated absorbing 'dust and polluted-dust' during the pre-monsoon season over the ICMR. Our result is corroborated with Manoj *et al* (2021) who reported a higher concentration of dust-dominated aerosols in the lower troposphere (altitude 1–4 km) over the central and eastern IGP. These types of elevated aerosol layers are frequently observed during premonsoon and monsoon onset period over this region (Mishra and Shibata 2012, Sarangi *et al* 2016, Manoj *et al* 2021).

3.2. Impact of aerosol on tropospheric thermal structure

Figure 2(a) shows the relationship between atmospheric daytime temperature (T_{day}) profiles and AOD over the study region. We observed significant reduction in temperature with increasing AOD at lower tropospheric pressure levels (viz., surface (black), 925 hPa (blue), and 850 hPa (red)). However, no such changes in T_{day} are observed at other pressure levels (700 hPa, 600 hPa, and 500 hPa). Similar results are observed in each year throughout the study period (figure S1). The highest average daytime instantaneous cooling (i.e. the product of $dT/d\tau$ and mean AOD shown in figure 2(a)) is observed at 925 hPa (-1.84 °C \pm 0.25 °C), followed by surface level (-1.30 °C \pm 0.18 °C) and minimum cooling at 850 hPa (-0.81 °C \pm 0.11 °C) in all 17 years (table S1). The incoming solar radiation directly interacts with the elevated aerosols which cause extinction by

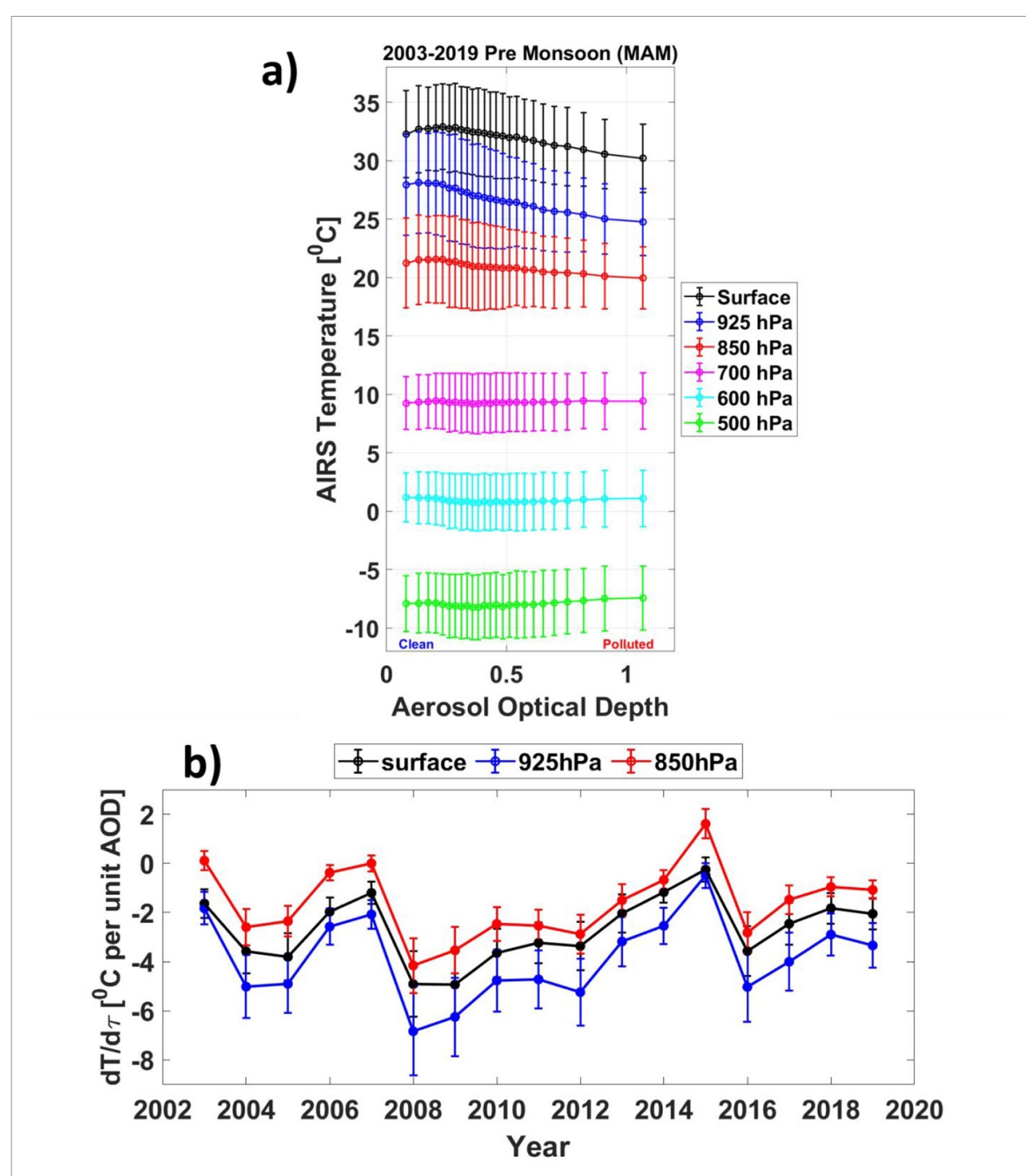


Figure 2. (a) AIRS derived atmospheric temperature profiles at six different pressure levels (surface: 925, 850, 700, 600 and 500 hPa) as a function of MODIS-AOD during the pre-monsoon season (MAM) for all 17 years from 2003 to 2019. Each bin contains four percentiles of all data (error bar shows standard deviation). (b) The time series of change in temperature per unit AOD ($dT/d\tau$) (°C per unit AOD) at surface, 925 and 850 hPa pressure levels, where each point shows the $dT/d\tau$ (error bars show the standard errors) for respective years.

absorption and scattering (aerosol-radiation interaction). This results in reduction of the amount of solar radiation reaching the surface, thereby causing cooling in the lower troposphere. We call this cooling as the aerosol direct effect. Though, the maximum cooling is expected at the surface rather than at 925 hPa, there are noises in surface signals due to surface heterogeneity and daytime convective buildup, which may bring error in calculation of surface emissivity and atmospheric corrected surface radiance recorded by AIRS (Divakarla *et al* 2006). Therefore, it may be related to the day-time artefacts in AIRS surface temperature retrieval (Divakarla *et al* 2006,

Maddy *et al* 2012). Nevertheless, consistent daytime instantaneous 'lower tropospheric cooling per unit AOD' ($dT/d\tau$) with significant interannual variability is observed from 2003 to 2019 (figure 2(b)). Our analysis (SN3) indicates that this variability in $dT/d\tau$ can be explained by the variability in chemical composition and size of ambient columnar aerosol loading. Using the annual $dT/d\tau$ values, we computed the daytime instantaneous aerosol-induced 'lower tropospheric cooling' over the ICMR during 2003–2019 (table S1). While maximum cooling is observed in the year 2008 (-3.38 °C \pm 0.46 °C at 925 hPa; -2.43 °C \pm 0.34 °C at the surface

and $-2.05~^{\circ}\text{C} \pm 0.28~^{\circ}\text{C}$ at 850 hPa), the minimum cooling is observed in 2015. At 850 hPa, statistically insignificant warming is observed in 2003 $(0.05~^{\circ}\text{C} \pm 0.09~^{\circ}\text{C})$ and 2015 $(0.80~^{\circ}\text{C} \pm 0.15~^{\circ}\text{C})$, whereas, the rest of the years are depicted with lower tropospheric cooling at all three levels. The observed warming in 2003 and 2005 can be explained as dominance of relatively smaller absorbing aerosols during these years as compared to others (SN3).

Further, the temperature fluctuations may also be governed by other unknown forcings such as regional scale circulation and other meteorological parameters (Quesada et al 2017, Guo et al 2020). Therefore, it is pertinent to rule out the influence of such variables on association between T and AOD. To address this concern, we performed partial correlation analysis (SN4, table S4). Our results show that the nature of the association between T and AOD still remains significantly negative even after removing the influence of meteorological variables. The possibility of non-physical artefacts due to latitudinal effect (SN5) is also ruled out. The time series analysis of averaged AOD and T over the ICMR shows that significant increase in AOD is associated with decrease in T at surface, 925 and 850 hPa (figure S6). It further testifies the strong negative association between AOD and T. To that end, our results indicate that lower tropospheric cooling may be due to the masking effect (aerosol direct effect) of aerosolradiation interaction (Mishra et al 2015, Sarangi et al

Though we are using quality controlled clearsky AOD and T_{day} products, the effect of cloud on AOD and atmospheric temperature retrieval cannot be ruled out in level 3 products (Lin et al 2014). Thus, the observed cooling trends in the lower troposphere may not be because of aerosol direct effect alone. There could be other factors such as aerosolcloud-radiation interaction (aerosol indirect effect) and cloud cooling effect, which may be playing role in the observed tropospheric cooling. Here, we refer to cloud cooling effect as the reduction in T_{day} due to changes in cloud properties which are not forced by variability in aerosols but by some other factors such as meteorology. Also, the cooling effects of aerosol loading can further affect cloud formation processes (Koren et al 2008, Rosenfeld et al 2008). Thus, we felt the need to examine the role of clouds in observed tropospheric cooling.

3.3. Role of clouds in observed tropospheric cooling

Figure 3(a) shows cloud classification and their frequency as a function of CF during the study period. It is seen that low-level clouds constitute more than 50% of all clouds (Cu=14.7%; SCu=34%; SC=4.9%). CF also increases as we move from low-level clouds to high-level clouds (mainly DCC) over the region. Figure 3(a) also shows that the maximum cloud

frequency (more than 65%) is associated with cloud cover less than 0.5, which can be treated as an ambient (most common) cloud cover condition in our study. The slope of 'AOD vs T' association, i.e. $\mathrm{d}T/\mathrm{d}\tau$ shows the change in temperature per unit change in AOD. The positive value of $\mathrm{d}T/\mathrm{d}\tau$ shows warming, whereas the negative value shows cooling. We observed that $\mathrm{d}T/\mathrm{d}\tau$ increases (in magnitude) when CF increases at both 925 hPa and 850 hPa levels (figure 3(b)). It is also observed that $\mathrm{d}T/\mathrm{d}\tau$ is slightly positive (though statistically insignificant) at 850 hPa in clear sky conditions. This hints towards absorbing aerosols induced radiative heating during clear sky conditions at this level.

Almost similar pattern is observed for individual years during 2003-2019 as well (figure S7). In general, our results indicate the intensification of aerosolinduced tropospheric cooling with increase in cloud coverage. A possible physical mechanism could be the enhancement of cloud brightening under high aerosol loading, which decreases the solar radiation reaching the lower troposphere. Similar associations are reported by Sarangi et al (2018) during monsoon season using numerical and radiative models. However, the increase in $dT/d\tau$ with increase in cloudiness may be caused not just by aerosol indirect effect, but also by cloud cooling effect. Due to nonlinear association between aerosol-cloud-radiation interactions, removing cloud cooling effect is challenging. We have tried to partially constrain this issue by removing CF above 0.5 data in our analysis.

The tropospheric temperature profiles are the net result of different parameters (e.g. solar and thermal radiation fluxes, greenhouse gases and aerosol concentrations, associated convective currents) and their interactions (Stephens and L'Ecuyer 2015, Seinfeld and Pandis 2016). Examining the variations in downwelling SW and LW radiation fluxes at the surface with AOD in both clear-sky and all-sky conditions may provide more insight into the observed cooling. Figure 3(c) shows the variation of downwelling SW and LW fluxes with AOD in clear-sky and allsky conditions. It is clearly seen that all-sky and clearsky SW radiation fluxes (green and cyan, respectively) decrease with increased aerosol loading. On the other hand, all-sky and clear-sky downwelling LW radiation fluxes (blue and red, respectively) increase with the increased aerosol loading. We observed that the difference between downwelling LW and SW radiation fluxes is less during clear-sky conditions than that during all-sky conditions. The difference between LW all-sky and LW clear-sky stays almost constant as a function of AOD. However, the downwelling SW reduction is more pronounced in all-sky conditions than that in clear sky conditions as a function of AOD, especially in polluted scenarios (AOD > 0.5). This analysis indicates that ambient cloud conditions assist the aerosol-induced SW cooling more as compared to LW warming. In general, the low-level clouds are

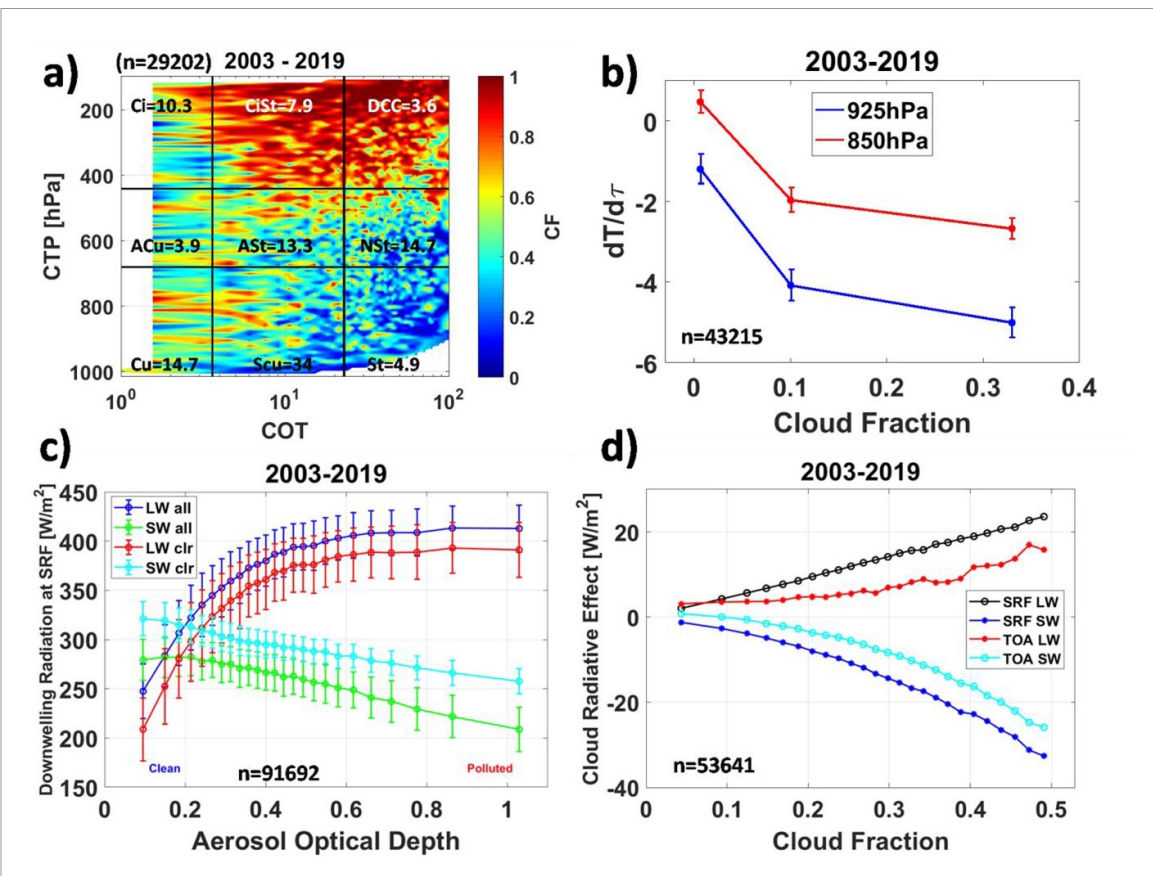


Figure 3. (a) Cloud-type classification derived from MODIS data as a function of CF. The frequencies of respective clouds are shown with cloud types. (b) Change in air temperature per unit AOD $(dT/d\tau)$ as a function of cloud fraction (for CF < 0.5). The total number of data is divided into three equal percentiles, where each point shows $dT/d\tau$ in respective CF ranges with error bars (standard slope errors). (c) Downwelling all-sky and clear-sky incoming SW and LW radiation at SRF as a function of AOD, and (d) CRE for both SW and LW at the SRF as well as TOA as a function of CF during the pre-monsoon season for 17 years from 2003 to 2019 over the ICMR. Each bin contains four percentiles of all data (figures (c) and (d)) with an error bar showing half standard deviation (figure (c)). The total number of data samples used in various analyses are shown as 'n' in respective plots.

mainly associated with SW cooling as compared to their LW warming effect (Kang *et al* 2020), which is also seen in our observations. Maharana *et al* (2019) explained a 2 °C–2.5 °C reduction of 2 m air temperature over central India during pre-monsoon season as a result of blocking of incoming SW radiation by dust aerosols.

To further examine the effect of clouds in the lower tropospheric cooling, we analyzed (figure 3(d)) the variation in CRE with respect to CF for both LW and SW, at SRF and TOA. While the LW-CRE increases with CF, the SW-CRE decreases with CF. However, the decrease of SW-CRE with CF is far more pronounced than the increase in LW-CRE. This clearly indicates that SW reduction is more compared to LW increase at the SRF, which is also reported by Saud *et al* (2016). Thus, our analysis shows the effect of CF on $\mathrm{d}T/\mathrm{d}\tau$ is the result of competing radiative effects of clouds in SW and LW regimes and clouds intensify the observed aerosol-induced lower tropospheric cooling.

Overall, we find that our results are manifestation of the direct and indirect radiative effect of aerosols on the thermal structure. Sarangi *et al* (2018) observed net negative CRE at both SRF and TOA over

the Indian summer monsoon region during the monsoon season. Zhu *et al* (2007) also showed net negative CRE at the surface due to elevated multilayer dust aerosols. A spatial variation in the sign of direct radiative effect of dust is found on a global scale but overall dust promotes cooling at the surface (di Biagio *et al* 2020). Thus, we find that 'dust and polluted-dust' with ambient cloud cover play a major role in observed aerosol-induced lower tropospheric cooling over the ICMR.

This study mainly reports observational findings of robust aerosol-induced instantaneous daytime lower tropospheric cooling during the pre-monsoon season. Further, we analyzed aerosol-cloud-radiation-temperature variability to infer that the observed daytime lower tropospheric cooling is the result of both direct radiative processes from elevated layers or/and aerosol-cloud-radiation interactionprocesses. Along with advection, the ambient temperature varies due to variation in tendency of microphysical, boundary layer, diabatic, aerosol and convective processes etc. The offline radiative transfer models (RTMs) simulate plane-parallel extinction of solar radiation as they interact with different layers of aerosols and clouds. Thus, they can be used to obtain

instantaneous radiative forcing at different layers and associated heating rates. Many previous studies over north India have used RTMs to calculate the aerosol direct radiative forcing and heating rates during premonsoon period (as mentioned in our section 1). Our results are consistent with the understanding of these previous studies based on offline RTM simulations (Singh et al 2004, Prasad et al 2007, Bibi et al 2017, Verma et al 2017). However, the estimation of sensitivity of temperature to aerosols is not appropriate in offline RTMs as they need assumption of radiative equilibrium conditions, which has a lot of uncertainties. Further, the aerosol-temperature processes involve complex nonlinear aerosol-cloud-radiationtemperature feedbacks and processes, which are missing in these offline simulations. Thus, RTM-based examination of our findings requires sophisticated coupled simulations and segregation of the contributions from various other confounding factors, which is beyond the scope of this present study.

3.4. Dynamical impact of lower tropospheric cooling

The observed cooling is consistent throughout the study period (2003-2019). The lower tropospheric stability (LTS, in °C) is defined as the difference between the potential temperatures at two different pressure levels in lower troposphere (Wood and Bretherton 2006). Here we have calculated the LTS using AIRS-derived potential temperature differences between 700 hPa and 925 hPa levels. Figure 4(a) shows the LTS as a function of AOD (black line), where each black color-filled circles present mean of four percentiles. The yellow color circles represent the potential temperature differences between 700 hPa and 925 hPa. Results indicate that the lower troposphere below 700 hPa gets stable as the aerosol loading increases. Similar kind of LTS is observed due to diabatic heating of elevated absorbing aerosols over Kanpur, a city in the polluted IGP (Sarangi et al 2016) and the eastern Mediterranean basin (Mishra et al 2014). Dipu et al (2013) have shown the effect of elevated dust layers on precipitation pattern and cloud formation as a result of surface fluxes reduction and boundary layer stabilization. The stable atmosphere causes the pollution layer to be stagnant in the boundary layer. This stabilized lower troposphere increases the probability of the aerosol layer formation in the lower troposphere which further promotes lower tropospheric cooling, a positive feedback.

The observed LTS may affect the cloud formation processes and their frequency over the study region. Figure 4(b) shows the cloud frequency (in %) as a function of AOD for the period 2003–2019. Frequency of low-level clouds (blue line) increases and the frequency of mid-level (red line) and high-level clouds (black line) decreases with AOD. The frequency of all three types of low-level, mid-level and high-level clouds has been shown in

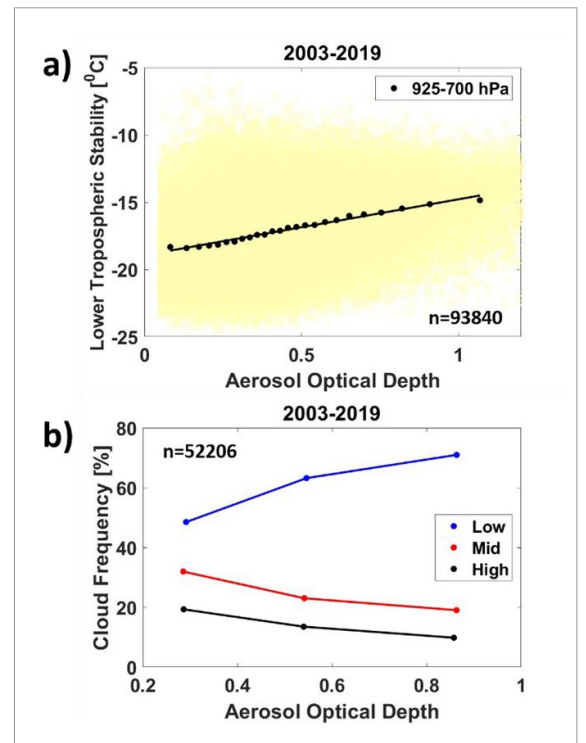


Figure 4. (a) LTS as a function of aerosol loading for the 925 hPa and 700 hPa. Background yellow circles show entire data for respective pressure levels. The black color-filled circles contain four percentiles of all data. (b) Frequency of cloud types (low, mid, high) as a function of AOD (for 5–30 percentiles, 40–65 percentiles, and 70–95 percentiles AOD). The total number of data samples used in various analyses are shown as 'n' in respective plots.

supplementary figure S8. It shows that the frequencies of cumulus (Cu) and stratocumulus (Scu) are increasing whereas frequencies of all other cloud types are decreasing with AOD (figure S8(a)). This variation in cloud frequency as a function of aerosols can be due to aerosol-cloud interaction, aerosol-cloud-climate interactions, etc, which may also affect the other cloud properties.

Using numerical model simulations, Perlwitz and Miller (2010) have shown that the radiative heating by highly absorbing elevated dust layers may enhance moisture convergence, and increase specific humidity in the lower troposphere during the pre-monsoon season. It leads to an increase in low cloud cover. This is in agreement with our results that highlights the increase in low cloud cover as a consequence of increased extinction caused by dust/polluted-dust during pre-monsoon. Using a regional climate model, Das et al (2015) have shown that stronger monsoon winds of 2010 brought higher dust aerosols over the IGP, which resulted in higher negative SW radiative forcing at SRF. Further, the diabatic heating associated with high AOD caused strengthening of zonal wind, which facilitated cloud formation at 850 hPa above the aerosol layer (Das et al 2015). The increase in low cloud cover as a function of aerosol loading further needs to be investigated in view of changing thermodynamics and biophysical parameters as a feedback of the observed effect of aerosol-cloudradiation interaction over the region.

4. Conclusions

The present study analyzed lower tropospheric temperature changes due to aerosol loading and associated mechanisms over the ICMR using 17 years (2003-2019) multi-satellite and ground-based observations during the pre-monsoon season. We found the decrease in lower tropospheric temperature (surface to 850 hPa) as a function of AOD, whereas no such changes are observed at higher altitudes (700-500 hPa). Results show consistent signature of temperature sensitivity to AOD $(dT/d\tau)$ i.e. instantaneous daytime cooling per unit AOD is observed in all years, with significant interannual variability in magnitude. This variability in $dT/d\tau$ is associated with annual changes in aerosol chemical and physical properties, reflected through the changes in SSA and AE. The radiometer and lidar data analysis show the dominance of elevated dust and polluted-dust (mixed) layers, which are predominantly responsible for observed instantaneous 'lower tropospheric cooling'. Further, our analyses ruleout the impact of variations of meteorological and cloud properties (except CF) on the observed association between AOD and T. At first glance, the observed cooling can be seen as aerosol direct effect (aerosol-radiation interaction) i.e. extinction of solar radiation due to scattering/absorption by aloft aerosol layers. However, after examining the effect of cloud cover, we found that the observed aerosol-induced lower tropospheric cooling enhances as a function of cloudiness. In other words, aerosol induced increase in cloudiness (aerosol indirect effect) further intercepts more solar radiation and increases the lower tropospheric cooling (i.e. aerosolcloud-radiation interaction). The aerosol induced (direct and indirect effect) cooling in polluted conditions stabilizes the lower troposphere. The dynamical response of observed cooling was seen as changes in occurrence of different cloud types over the region, which necessitates further investigations to understand aerosol-cloud-radiation-dynamics feedback mechanisms.

Data availability statement

All data that supports the findings of this study are included in the article and supplementary materials. Raw data from AERONET, AIRS, MODIS, CALIPSO and CERES can be downloaded from respective agencies. Additional data/code requirement may be requested from the authors.

Author's contributions

A K M and I K conceptualize and M J and A K M designed it. M J developed the algorithm and analyzed

the data. C S, I K, K K, S S and S N T provided important inputs in analysis. M J and A K M have drafted the manuscript with revision from C S, I K, K K, S S, and S N T. All authors contributed to interpretation and discussion of the results.

Acknowledgments

One of the authors (A K M) would like to thank the DST Purse Grant and DST INSPIRE Faculty Grant [DST/INSPIRE/04/2015/003253] for providing the necessary funds for conducting the study. A K M and M J would also like to thank Jawaharlal Nehru University, New Delhi for providing necessary resources to conduct this study. Further, authors would like to thanks the team members of AERONET, AIRS, MODIS, CALIPSO and CERES for maintaining and providing various datasets used in this study. We are thankful to the anonymous referees for their valuable comments and suggestions to improve this paper.

Conflict of interest

The authors declare that they have no conflict of interests.

ORCID iDs

Manish Jangid 6 https://orcid.org/0000-0002-6977-7470

Amit Kumar Mishra https://orcid.org/0000-0002-4620-2631

References

Albrecht B A 1989 Aerosols, cloud microphysics, and fractional cloudiness *Science* 245 1227–30

Bibi H, Alam K and Bibi S 2017 Estimation of shortwave direct aerosol radiative forcing at four locations on the Indo-Gangetic plains: model results and ground measurement *Atmos. Environ.* **163** 166–81

Boucher O et al 2013 Clouds and aerosols Climate Change 2013: The Physical Science Basis. Contribution of Working Group I to the Fifth Assessment Report of the Intergovernmental Panel on Climate Change (Cambridge: Cambridge University Press) pp 571–657

Cairo F, Donfrancesco G D, Adriani A, Pulvirenti L and Fierli F 1999 Comparison of various linear depolarization parameters measured by lidar *Appl. Opt.* 38 4425

D'Errico M, Cagnazzo C, Fogli P G, Lau W K, von Hardenberg J, Fierli F and Cherchi A 2015 Indian monsoon and the elevated-heat-pump mechanism in a coupled aerosol-climate model *J. Geophys. Res. Atmos.* 120 8712–23

Das S, Dey S and Dash S K 2015 Impacts of aerosols on dynamics of Indian summer monsoon using a regional climate model *Clim. Dyn.* 44 1685–97

Davidi A, Koren I and Remer L 2009 Direct measurements of the effect of biomass burning over the Amazon on the atmospheric temperature profile *Atmos. Chem. Phys.* 9 8211–21

Davidi A, Kostinski A B, Koren I and Lehahn Y 2012 Observational bounds on atmospheric heating by aerosol

- absorption: radiative signature of transatlantic dust *Geophys*. Res. Lett. 39
- di Biagio C, Balkanski Y, Albani S, Boucher O and Formenti P 2020 Direct radiative effect by mineral dust aerosols constrained by new microphysical and spectral optical data Geophys. Res. Lett. 47 e2019GL086186
- Dipu S, Prabha T V, Pandithurai G, Dudhia J, Pfister G, Rajesh K and Goswami B N 2013 Impact of elevated aerosol layer on the cloud macrophysical properties prior to monsoon onset *Atmos. Environ.* **70** 454–67
- Divakarla M G, Barnet C D, Goldberg M D, McMillin L M, Maddy E, Wolf W, Zhou L and Liu X 2006 Validation of Atmospheric Infrared Sounder temperature and water vapor retrievals with matched radiosonde measurements and forecasts J. Geophys. Res. Atmos. 111 D09S15
- Feingold G, McComiskey A, Yamaguchi T, Johnson J S, Carslaw K S and Schmidt K S 2016 New approaches to quantifying aerosol influence on the cloud radiative effect *Proc. Natl Acad. Sci.* 113 5812–9
- Fu Q, Johanson C M, Warren S G and Seidel D J 2004 Contribution of stratospheric cooling to satellite-inferred tropospheric temperature trends *Nature* 429 55–58
- Ganguly D, Rasch P J, Wang H and Yoon J-H 2012 Climate response of the South Asian monsoon system to anthropogenic aerosols *J. Geophys. Res. Atmos.* 117 D13209
- Gargava P and Aggarwal A L 1996 Industrial emissions in a coastal region of India: prediction of impact on air environment Environ. Int. 22 361–7
- Garrett T J and Zhao C 2006 Increased Arctic cloud longwave emissivity associated with pollution from mid-latitudes Nature 440 787–9
- Gautam R *et al* 2011 Accumulation of aerosols over the Indo-Gangetic plains and southern slopes of the Himalayas: distribution, properties and radiative effects during the 2009 pre-monsoon season *Atmos. Chem. Phys.* 11 12841–63
- Giles D M, Holben B N, Eck T F, Sinyuk A, Smirnov A, Slutsker I, Dickerson R R, Thompson A M and Schafer J S 2012 An analysis of AERONET aerosol absorption properties and classifications representative of aerosol source regions *J. Geophys. Res. Atmos.* 117 D17203
- Guo J *et al* 2020 The climatology of lower tropospheric temperature inversions in China from radiosonde measurements: roles of black carbon, local meteorology, and large-scale subsidence *J. Clim.* 33 9327–50
- Holben B N *et al* 1998 AERONET-A federated instrument network and data archive for aerosol characterization *Remote Sens. Environ.* **66** 1–16
- Höpner F, Bender F M, Ekman A M, Andersson A, Gustafsson Ö and Leck C 2019 Investigation of two optical methods for aerosol-type classification extended to a Northern Indian Ocean site *J. Geophys. Res. Atmos.* 124 8743–63
- Jangid M, Chaubey S and Mishra A K 2019 A study of optical and microphysical properties of atmospheric brown clouds Measurement, Analysis and Remediation of Environmental Pollutants 1 Gupta T, Singh P S, Rajput P and Agrawal K A Energy, Environment, and Sustainability (Singapore: Springer) p 179–98
- Kandlikar M and Ramachandran G 2000 The causes and consequences of particulate air pollution in urban India: a synthesis of the science Annu. Rev. Energy Environ. 25 629–84
- Kang H, Choi Y-S, Hwang J and Kim H-S 2020 On the cloud radiative effect for tropical high clouds overlying low clouds *Geosci. Lett.* 7 1–6
- Kaskaoutis D G et al 2012 Influence of anomalous dry conditions on aerosols over India: transport, distribution and properties J. Geophys. Res. 117 D09106
- Koren I, Martins J V, Remer L A and Afargan H 2008 Smoke invigoration versus inhibition of clouds over the Amazon Science 321 946–9
- Kothawale D R and Kumar K R 2002 Tropospheric temperature variation over India and links with the Indian summer monsoon: 1971–2000 *Mausam* 53 289–308

- Kovilakam M and Mahajan S 2016 Confronting the "Indian summer monsoon response to black carbon aerosol" with the uncertainty in its radiative forcing and beyond *J. Geophys. Res. Atmos.* 121 7833–52
- Krishnamohan K S, Modak A and Bala G 2021 Effects of local and remote black carbon aerosols on summer monsoon precipitation over India Environ. Res. Commun. 3 081003
- Kulkarni P, Ramachandran S, Bhavani Kumar Y, Narayana Rao D and Krishnaiah M 2008 Features of upper troposphere and lower stratosphere aerosols observed by lidar over Gadanki, a tropical Indian station *J. Geophys. Res. Atmos.* **113** D17207
- Kumar S and Bhat G S 2016 Vertical profiles of radar reflectivity factor in intense convective clouds in the tropics *J. Appl. Meteorol. Climatol.* 55 1277–86
- Kuttippurath J and Raj S 2021 Two decades of aerosol observations by AATSR, MISR, MODIS and MERRA-2 over India and Indian Ocean *Remote Sens. Environ.* **257** 112363
- Lau K M, Kim M K and Kim K M 2006 Asian summer monsoon anomalies induced by aerosol direct forcing: the role of the Tibetan Plateau Clim. Dyn. 26 855–64
- Lau K-M and Kim K-M 2006 Observational relationships between aerosol and Asian monsoon rainfall, and circulation Geophys. Res. Lett. 33 L21810
- Li W, Shao L, Zhang D, Ro C-U, Hu M, Bi X, Geng H, Matsuki A, Niu H and Chen J 2016a A review of single aerosol particle studies in the atmosphere of East Asia: morphology, mixing state, source, and heterogeneous reactions *J. Clean. Prod.* 112 leel 330–49
- Li Z et al 2016b Aerosol and monsoon climate interactions over Asia Rev. Geophys. 54 866–929
- Liang Y, Sun X, Miller S D, Li H, Zhou Y, Zhang R and Li S 2017 Cloud base height estimation from ISCCP cloud-type classification applied to A-train data Adv. Meteorol. 2017 3231719
- Lin J, van Donkelaar A, Xin J, Che H and Wang Y 2014 Clear-sky aerosol optical depth over East China estimated from visibility measurements and chemical transport modeling Atmos. Environ. 95 258–67
- Loeb N G, Doelling D R, Wang H, Su W, Nguyen C, Corbett J G, Liang L, Mitrescu C, Rose F G and Kato S 2018 Clouds and the earth's radiant energy system (CERES) energy balanced and filled (EBAF) top-of-atmosphere (TOA) edition-4.0 data product *J. Clim.* 31 895–918
- Maddy E S *et al* 2012 On the effect of dust aerosols on AIRS and IASI operational level 2 products *Geophys. Res. Lett.* **39** L10809
- Maddy E S and Barnet C D 2008 Vertical Resolution Estimates in Version 5 of AIRS Operational Retrievals *IEEE Trans. Geosci. Remote Sensing* 46 2375–84
- Maharana P, Dimri A P and Choudhary A 2019 Redistribution of Indian summer monsoon by dust aerosol forcing *Meteorol*. Appl. 26 584–96
- Manoj M R, Satheesh S K, Moorthy K K, Trembath J and Coe H 2021 Measurement report: altitudinal variation of CCN activation across the Indo-Gangetic plains prior to monsoon onset and during peak monsoon periods: results from the SWAAMI field campaign *Atmos. Chem. Phys. Discuss.* 21 8979–97
- Mhawish A *et al* 2021 Aerosol characteristics from earth observation systems: a comprehensive investigation over South Asia (2000–2019) *Remote Sens. Environ.* **259** 112410
- Mishra A K, Klingmueller K, Fredj E, Lelieveld J, Rudich Y and Koren I 2014 Radiative signature of absorbing aerosol over the eastern Mediterranean Basin *Atmos. Chem. Phys.* 14 7213–31
- Mishra A K, Koren I and Rudich Y 2015 Effect of aerosol vertical distribution on aerosol-radiation interaction: a theoretical prospect *Heliyon* 1 e00036 (PMID: 27441222 PMCID: PMC4939813)
- Mishra A K and Shibata T 2012 Climatological aspects of seasonal variation of aerosol vertical distribution over central Indo-Gangeticbelt (IGB) inferred by the space-borne lidar CALIOP *Atmos. Environ.* 46 365–75

- Nigam S and Bollasina M 2010 "Elevated heat pump" hypothesis for the aerosol-monsoon hydroclimate link: "Grounded" in observations? J. Geophys. Res. Atmos. 115 D16201
- Omar A H *et al* 2009 The CALIPSO automated aerosol classification and lidar ratio selection algorithm *J. Atmos. Ocean. Technol.* **26** 1994–2014
- Pandey S K, Vinoj V, Landu K and Babu S S 2017 Declining pre-monsoon dust loading over South Asia: signature of a changing regional climate *Sci. Rep.* 7 1–10
- Perlwitz J and Miller R L 2010 Cloud cover increase with increasing aerosol absorptivity: a counterexample to the conventional semidirect aerosol effect J. Geophys. Res. Atmos. 115 D08203
- Prasad A K, Singh S, Chauhan S S, Srivastava M K, Singh R P and Singh R 2007 Aerosol radiative forcing over the Indo-Gangetic plains during major dust storms *Atmos. Environ.* 41 6289–301
- Quesada B, Arneth A and de Noblet-ducoudré N 2017 Atmospheric, radiative, and hydrologic effects of future land use and land cover changes: a global and multimodel climate picture *J. Geophys. Res. Atmos.* 122 5113–31
- Ramanathan R and Parikh J K 1999 Transport sector in India: an analysis in the context of sustainable development *Transp. Policy* 6 35–45
- Ramanathan V 2004 Atmospheric brown clouds: health, climate and agriculture impacts Scripta Varia **106** Working Group 31 Oct - 2 Nov 2004 (Vatican City: Pontifica Academia Scientiarym) p 47–60
- Ramanathan V, Chung C, Kim D, Bettge T, Buja L, Kiehl J T, Washington M, Fu Q, Sikka D R and Wild M 2005
 Atmospheric brown clouds: impacts on South Asian climate and hydrological cycle *Proc. Natl Acad. Sci.* 102 5326–33
- Ramanathan V and Crutzen P J 2003 New directions: atmospheric brown clouds *Atmos. Environ.* **37** 4033–5
- Ramanathan V and Feng Y 2009 Air pollution, greenhouse gases and climate change: global and regional perspectives *Atmos. Environ.* **43** 37–50
- Rosenfeld D, Woodley W L, Axisa D, Freud E, Hudson J G and Givati A 2008 Aircraft measurements of the impacts of pollution aerosols on clouds and precipitation over the Sierra Nevada *J. Geophys. Res.* 113 D15203
- Ross R S, Krishnamurti T N, Pattnaik S and Pai D S 2018 Decadal surface temperature trends in India based on a new high-resolution data set *Sci. Rep.* 8 1–10
- Rossow W B and Schiffer R A 1991 ISCCP cloud data products Bull. Am. Meteorol. Soc. 72 2–20
- Russell P B, Bergstrom R W, Shinozuka Y, Clarke A D, DeCarlo P F, Jimenez J L, Livingston J M, Redemann J, Dubovik O and Strawa A 2010 Absorption Ångström exponent in AERONET and related data as an indicator of aerosol composition Atmos. Chem. Phys. 10 1155–69
- Saha S B, Roy S S, Bhowmik S K and Kundu P K 2014
 Intra-seasonal variability of cloud amount over the Indian subcontinent during the monsoon season as observed by TRMM precipitation radar *Geofizika* 31 29–53
- Sarangi C, Kanawade V P, Tripathi S N, Thomas A and Ganguly D 2018 Aerosol-induced intensification of cooling effect of clouds during Indian summer monsoon *Nat. Commun.* 9 1–9
- Sarangi C, Tripathi S N, Mishra A K, Goel A and Welton E J 2016 Elevated aerosol layers and their radiative impact over Kanpur during monsoon onset period *J. Geophys. Res. Atmos.* 121 7936–57
- Saud T, Dey S, Das S and Dutta S 2016 A satellite-based 13-year climatology of net cloud radiative forcing over the Indian monsoon region Atmos. Res. 182 76–86
- Seinfeld J H and Pandis N 2016 Atmospheric Chemistry and Physics: From Air Pollution to Climate Change (NY: Wiley)
- Shupe M D and Intrieri J M 2004 Cloud radiative forcing of the Arctic surface: the influence of cloud properties, surface albedo, and solar zenith angle J. Clim. 17 616–28

- Singh R P, Dey S, Tripathi S N, Tare V and Holben B 2004 Variability of aerosol parameters over Kanpur, northern India *J. Geophys. Res. Atmos.* **109** D23206
- Singh S, Soni K, Bano T, Tanwar R S, Nath S and Arya B C 2010 Clear-sky direct aerosol radiative forcing variations over mega-city Delhi *Ann. Geophys.* 28 1157–66
- Smirnov A, Holben B N, Kaufman Y J, Dubovik O, Eck T F, Slutsker I, Pietras C and Halthore R N 2002 Optical properties of atmospheric aerosol in maritime environments *J. Atmos. Sci.* **59** 501–23
- Smith G L, Mlynczak P E and Potter G L 2012 A technique using principal component analysis to compare seasonal cycles of Earth radiation from CERES and model computations *J. Geophys. Res. Atmos.* 117 D09116
- Soni K, Singh S, Bano T, Tanwar R S and Nath S 2011 Wavelength dependence of the aerosol Angstrom exponent and its implications over Delhi, India Aerosol Sci. Technol. 45 1488–98
- Stapf J, Ehrlich A, Jäkel E, Lüpkes C and Wendisch M 2020 Reassessment of shortwave surface cloud radiative forcing in the Arctic: consideration of surface-albedo–cloud interactions *Atmos. Chem. Phys.* **20** 9895–914
- Stephens G L and L'Ecuyer T 2015 The Earth's energy balance Atmos. Res. 166 195–203
- Thomas A, Sarangi C and Kanawade V P 2019 Recent increase in winter Hazy days over central india and the Arabian Sea *Sci. Rep.* 9 1–10
- Tripathi S N, Dey S, Tare V and Satheesh S K 2005a Aerosol black carbon radiative forcing at an industrial city in Northern India *Geophys. Res. Lett.* **32** L08802
- Tripathi S N, Dey S, Tare V, Satheesh S K, Lal S and Venkataramani S 2005b Enhanced layer of black carbon in a north Indian industrial city *Geophys. Res. Lett.* **32** L12802
- Twomey S 1977 The influence of pollution on the shortwave albedo of clouds J. Atmos. Sci. 34 1149–52
- Verma S, Prakash D, Srivastava A K and Payra S 2017 Radiative forcing estimation of aerosols at an urban site near the thar desert using ground-based remote sensing measurements Aerosol Air Qual. Res. 17 1294–304
- Vernier J P, Fairlie T D, Natarajan M, Wienhold F G, Bian J, Martinsson B G, Crumeyrolle S, Thomason L W and Bedka K M 2015 Increase in upper tropospheric and lower stratospheric aerosol levels and its potential connection with Asian pollution *J. Geophys. Res. Atmos.* **120** 1608–19
- Winker D M, Hunt W H and McGill M J 2007 Initial performance assessment of CALIOP *Geophys. Res. Lett.* 34 L19803
- Winker D M, Pelon J and McCormick M P 2003 The CALIPSO mission: space borne lidar for observation of aerosols and clouds *Proc. SPIE 4893. Proc. Society of Photo-Optical Instrumentation* vol 1 pp 1–11
- Wonsick M M, Pinker R T and Ma Y 2014 Investigation of the "elevated heat pump" hypothesis of the Asian monsoon using satellite observations *Atmos. Chem. Phys.* 14 8749–61
- Wood R and Bretherton C S 2006 On the relationship between stratiform low cloud cover and lower-tropospheric stability *J. Clim.* 19 6425–32
- Young A S, Winker M D, Vaughan A M, Hu Y and Kuehn E R 2008 Cloud-aerosol lidar infrared pathfinder satellite observations CALIOP algorithm *Theoretical Basis Document* Document No: PC-SCI-202 part 4
- Young S A and Vaughan M A 2009 The retrieval of profiles of particulate extinction from cloud-aerosol lidar infrared pathfinder satellite observations (CALIPSO) data: algorithm description *J. Atmos. Ocean. Technol.* **26** 1105–19
- Zhao C, Yang Y, Fan H, Huang J, Fu Y, Zhang X, Kang S, Cong Z, Letu H and Menenti M 2020 Aerosol characteristics and impacts on weather and climate over the Tibetan Plateau Natl Sci. Rev. 7 492–5
- Zhu A, Ramanathan V, Li F and Kim D 2007 Dust plumes over the Pacific, Indian, and Atlantic oceans: climatology and radiative impact *J. Geophys. Res. Atmos.* 112 D16208